

# Measurement of the relative branching ratio $\text{BR}(\Xi_c^+ \rightarrow p^+ K^- \pi^+)/\text{BR}(\Xi_c^+ \rightarrow \Xi^- \pi^+ \pi^+)$

The FOCUS Collaboration

J. M. Link<sup>a</sup> M. Reyes<sup>a,1</sup> P. M. Yager<sup>a</sup> J. C. Anjos<sup>b</sup> I. Bediaga<sup>b</sup>  
 C. Göbel<sup>b,2</sup> J. Magnin<sup>b</sup> A. Massafferri<sup>b</sup> J. M. de Miranda<sup>b</sup>  
 I. M. Pepe<sup>b,3</sup> A. C. dos Reis<sup>b</sup> F. R. A. Simão<sup>b</sup> S. Carrillo<sup>c</sup>  
 E. Casimiro<sup>c,4</sup> A. Sánchez-Hernández<sup>c</sup> C. Uribe<sup>c,5</sup> F. Vázquez<sup>c</sup>  
 L. Cinquini<sup>d,6</sup> J. P. Cumalat<sup>d</sup> B. O'Reilly<sup>d</sup> J. E. Ramirez<sup>d</sup>  
 E. W. Vaandering<sup>d,7</sup> J. N. Butler<sup>e</sup> H. W. K. Cheung<sup>e</sup>  
 I. Gaines<sup>e</sup> P. H. Garbincius<sup>e</sup> L. A. Garren<sup>e</sup> E. Gottschalk<sup>e</sup>  
 P. H. Kasper<sup>e</sup> A. E. Kreymer<sup>e</sup> R. Kutschke<sup>e</sup> S. Bianco<sup>f</sup>  
 F. L. Fabbri<sup>f</sup> S. Sarwar<sup>f</sup> A. Zallo<sup>f</sup> C. Cawlfeld<sup>g</sup> D. Y. Kim<sup>g</sup>  
 A. Rahimi<sup>g</sup> J. Wiss<sup>g</sup> R. Gardner<sup>h</sup> Y. S. Chung<sup>i</sup> J. S. Kang<sup>i</sup>  
 B. R. Ko<sup>i</sup> J. W. Kwak<sup>i</sup> K. B. Lee<sup>i,8</sup> H. Park<sup>i</sup> G. Alimonti<sup>j</sup>  
 M. Boschini<sup>j</sup> B. Caccianiga<sup>j</sup> P. D'Angelo<sup>j</sup> M. DiCorato<sup>j</sup>  
 P. Dini<sup>j</sup> M. Giammarchi<sup>j</sup> P. Inzani<sup>j</sup> F. Leveraro<sup>j</sup> S. Malvezzi<sup>j</sup>  
 D. Menasce<sup>j</sup> M. Mezzadri<sup>j</sup> L. Milazzo<sup>j</sup> L. Moroni<sup>j</sup> D. Pedrini<sup>j</sup>  
 C. Pontoglio<sup>j</sup> F. Prelz<sup>j</sup> M. Rovere<sup>j</sup> A. Sala<sup>j</sup> S. Sala<sup>j</sup>  
 T. F. Davenport III<sup>k</sup> L. Agostino<sup>ℓ,9</sup> V. Arena<sup>ℓ</sup> G. Boca<sup>ℓ</sup>  
 G. Bonomi<sup>ℓ,10</sup> G. Gianini<sup>ℓ</sup> G. Liguori<sup>ℓ</sup> M. M. Merlo<sup>ℓ</sup>  
 D. Pantea<sup>ℓ,11</sup> S. P. Ratti<sup>ℓ</sup> C. Riccardi<sup>ℓ</sup> I. Segoni<sup>ℓ,9</sup> L. Viola<sup>ℓ</sup>  
 P. Vitulo<sup>ℓ</sup> H. Hernandez<sup>m</sup> A. M. Lopez<sup>m</sup> H. Mendez<sup>m</sup>  
 L. Mendez<sup>m</sup> A. Mirles<sup>m</sup> E. Montiel<sup>m</sup> D. Olaya<sup>m,9</sup> A. Paris<sup>m</sup>  
 J. Quinones<sup>m</sup> C. Rivera<sup>m</sup> W. Xiong<sup>m</sup> Y. Zhang<sup>m,12</sup>  
 J. R. Wilson<sup>n</sup> K. Cho<sup>o</sup> T. Handler<sup>o</sup> D. Engh<sup>p</sup> M. Hosack<sup>p</sup>  
 W. E. Johns<sup>p</sup> M. Nehring<sup>p,13</sup> P. D. Sheldon<sup>p</sup> K. Stenson<sup>p</sup>  
 M. Webster<sup>p</sup> M. Sheaff<sup>q</sup>

<sup>a</sup>*University of California, Davis, CA 95616*

<sup>b</sup>*Centro Brasileiro de Pesquisas Físicas, Rio de Janeiro, RJ, Brasil*

<sup>c</sup>*CINVESTAV, 07000 México City, DF, Mexico*

<sup>d</sup>*University of Colorado, Boulder, CO 80309*

<sup>e</sup>*Fermi National Accelerator Laboratory, Batavia, IL 60510*

<sup>f</sup>*Laboratori Nazionali di Frascati dell'INFN, Frascati, Italy I-00044*

<sup>g</sup>*University of Illinois, Urbana-Champaign, IL 61801*

<sup>h</sup>*Indiana University, Bloomington, IN 47405*

<sup>i</sup>*Korea University, Seoul, Korea 136-701*

<sup>j</sup>*INFN and University of Milano, Milano, Italy*

<sup>k</sup>*University of North Carolina, Asheville, NC 28804*

<sup>l</sup>*Dipartimento di Fisica Nucleare e Teorica and INFN, Pavia, Italy*

<sup>m</sup>*University of Puerto Rico, Mayaguez, PR 00681*

<sup>n</sup>*University of South Carolina, Columbia, SC 29208*

<sup>o</sup>*University of Tennessee, Knoxville, TN 37996*

<sup>p</sup>*Vanderbilt University, Nashville, TN 37235*

<sup>q</sup>*University of Wisconsin, Madison, WI 53706*

---

## Abstract

We report the observation of the Cabibbo suppressed decay  $\Xi_c^+ \rightarrow pK^-\pi^+$  using data collected with the FOCUS spectrometer during the 1996–97 Fermilab fixed target run. We find a  $\Xi_c^+$  signal peak of  $202 \pm 35$  events. We have measured the relative branching ratios  $\text{BR}(\Xi_c^+ \rightarrow pK^-\pi^+)/\text{BR}(\Xi_c^+ \rightarrow \Xi^-\pi^+\pi^+) = 0.234 \pm 0.047 \pm 0.022$  and  $\text{BR}(\Xi_c^+ \rightarrow p\bar{K}^*(892)^0)/\text{BR}(\Xi_c^+ \rightarrow pK^-\pi^+) = 0.54 \pm 0.09 \pm 0.05$ .

---

Much less is known about the decays and branching fractions of the charm baryons in comparison to the charm mesons; even less is known about charm

---

<sup>1</sup> Present Address: Instituto de Fisica y Matematicas, Universidad Michoacana de San Nicolas de Hidalgo, Morelia, Mich., Mexico 58040

<sup>2</sup> Present Address: Instituto de Física, Facultad de Ingeniería, Univ. de la República, Montevideo, Uruguay

<sup>3</sup> Present Address: Instituto de Física, Universidade Federal da Bahia, Salvador, Brazil

<sup>4</sup> Present Address: INFN sezione di Milano, Milano, Italy

<sup>5</sup> Present Address: Instituto de Física, Universidad Autónoma de Puebla,

<sup>6</sup> Present Address: National Center for Atmospheric Research, Boulder, CO

<sup>7</sup> Present Address: Vanderbilt University, Nashville, TN 37235

<sup>8</sup> Present Address: Korea Research Institute of Standards and Science, P.O.Box 102, Yusong-Ku, Taejon 305-600, South Korea

<sup>9</sup> Present Address: University of Colorado, Boulder 80309

<sup>10</sup> Present Address: Dipartimento di Chimica e Fisica per l'Ingegneria e per i Materiali, Università di Brescia and INFN sezione di Pavia

<sup>11</sup> Present Address: Nat. Inst. of Phys and Nucl. Eng., Bucharest, Romania

<sup>12</sup> Present Address: Lucent Technology

<sup>13</sup> Present Address: Adams State College, Alamosa, CO 81102

baryons containing strange quarks. In this article, we confirm the existence of the Cabibbo-suppressed decay of the  $\Xi_c^+$  baryon:  $\Xi_c^+ \rightarrow pK^-\pi^+$  (conjugate states should be implicitly assumed throughout this paper), which was observed for the first time only recently [1]. We also provide new information on the two-body decay  $\Xi_c^+ \rightarrow p\bar{K}^*(892)^0$ .

FOCUS is a high energy photo-production experiment at Fermilab designed to study charmed particle physics. Charmed hadrons were produced by the interaction of a photon beam on a beryllium oxide (BeO) target. Different target setups were used during the data taking; about 2/3 of the data were collected using a segmented BeO target interleaved with high resolution silicon detectors (TS). The decay products were reconstructed using a large acceptance multi-particle spectrometer. A vertex detector (SSD) composed of 12 planes of silicon was used to provide high resolution tracking in the region immediately downstream of the target, thus allowing the identification and separation of the charm production and decay vertices. Downstream of the SSD, tracking and momentum measurement were accomplished with five stations of multi-wire proportional chambers and two large aperture magnets operated with opposite polarity. Three multi-cell Čerenkov counters operating in threshold mode allowed identification of charged electrons, pions, kaons, and protons over a large momentum range. The spectrometer also contained a hadron calorimeter, two electromagnetic calorimeters, and two muon detectors.

Events were selected which contained at least one identified proton track, one kaon track, and one pion track. The proton and pion had the same charge while the kaon had an opposite charge.

Due to *a priori* likelihoods, the tightest Čerenkov cuts were placed on the proton, the loosest cuts on the pion. The proton candidate was selected by requiring that the proton hypothesis was favored (by the Čerenkov analysis algorithm) over both the kaon and pion hypotheses by 0.7 and 4.0 units of likelihood, respectively. The kaon candidate was selected by requiring the kaon hypothesis to be favored over the pion hypothesis by 2.5 units of likelihood and not disfavoured by the proton hypothesis by more than 1 unit of likelihood. For the pion candidate, we required that the pion hypothesis was within 8.0 units of likelihood of the most likely hypothesis. A more detailed discussion of the Čerenkov analysis algorithm may be found elsewhere [2]. All the candidate particles were also required to be inconsistent with a muon hypothesis using the muon detectors and also to be inconsistent with an electron-positron pair. Furthermore kaon candidates were required to have a momentum greater than 8 GeV/c.

Known meson reflections where another particle was misidentified as the proton were reduced by raising Čerenkov requirements on the proton candidate for combinations compatible with the decay modes  $(D_s^{+*}), D^+, D_s^+ \rightarrow K^+K^-\pi^+$ ,

and  $D^+ \rightarrow K^- \pi^+ \pi^+$ . A significant background contribution from  $\phi(1020) \rightarrow K^+ K^-$  was suppressed in the same manner.

The process  $\Xi_c^+ \rightarrow \Xi^- \pi^+ \pi^+$  has been selected as the normalization channel. For this decay pions have been subjected to similar Čerenkov cuts to reduce systematics, while  $\Xi^-$  hyperons were fully reconstructed via the channel  $\Xi^- \rightarrow \Lambda^0 \pi^-$ . The  $\Lambda\pi$  invariant mass was required to fall within three standard deviation of the known  $\Xi^-$  mass.

After the candidate tracks were selected, the event was reconstructed using a candidate driven vertex algorithm which is described in detail elsewhere [3]. The algorithm forms a secondary vertex from the candidate tracks and uses the total momentum vector as a seed to construct a primary vertex by intersecting the seed with other tracks in the event. The procedure returns the confidence level of the fits for the secondary (CLS) and primary (CLP) vertices plus the detachment significance between the two,  $\ell/\sigma_\ell$ , where  $\ell$  is the distance between the vertices and  $\sigma_\ell$  is its error. In this analysis, the  $\ell/\sigma_\ell$  variable is the most powerful tool in extracting the charm signal from the background. The same algorithm also returns an estimator of the relative isolation of the obtained vertices. This estimator (ISO1) is the confidence level that tracks forming the secondary vertex might instead come from the primary vertex. The described set of variables provides a good description of the topological configuration of the event such that an appropriate set of cuts on them effectively rejects the background.

We require  $\ell/\sigma_\ell > 8$  as a compromise between the requirements to have good statistics and a good signal to noise ratio. The same vertexing cuts,  $\text{CLS} \geq 1\%$ ,  $\text{CLP} \geq 1\%$ , and  $\text{ISO1} < 95\%$  were used for both the Cabibbo suppressed channel and the normalization channel. For the Cabibbo suppressed decay we further require the proper time resolution of the candidate to be less than 75 fs. Also, the primary vertex is required to have at least two tracks in addition to the charm seed.

Using these selection criteria, we obtain the mass plots for the  $pK^- \pi^+$  and  $\Xi^- \pi^+ \pi^+$  combinations shown in Figure 1 (a,b) respectively. In Figure 1 (a) the signal is clearly visible in the inset while in the full view the  $\Lambda_c^+ \rightarrow pK^- \pi^+$  mode dominates. The fit to the invariant mass distribution is performed with a Gaussian function for the  $\Xi_c^+ \rightarrow pK^- \pi^+$  signal and a straight line for the background. In Figure 1 (b) the fit to the  $\Xi^- \pi^+ \pi^+$  invariant mass distribution is also performed using a Gaussian signal and a linear background. The fits yield  $202 \pm 35$  events for the  $\Xi_c^+ \rightarrow pK^- \pi^+$  channel and  $133 \pm 14$  events for the  $\Xi_c^+ \rightarrow \Xi^- \pi^+ \pi^+$  channel. A cleaner sample for the  $\Xi_c^+ \rightarrow pK^- \pi^+$  can be achieved, as shown in Figure 2, by means of tighter Čerenkov cuts and a tighter requirement on the detachment significance  $\ell/\sigma_\ell$ .

The efficiencies for the two decay modes were determined using a Monte Carlo simulation. The efficiency ratio for the two modes was found to be  $\varepsilon_{\Xi^-\pi^+\pi^+}/\varepsilon_{pK^-\pi^+} = 0.1539 \pm 0.0033$ . Correcting by this factor, the branching ratio is calculated to be  $0.234 \pm 0.047$  (statistical error only).

Extensive systematic studies and consistency checks were performed on the branching ratio measurement. The behaviour of the  $\Xi_c^+ \rightarrow pK^-\pi^+$  and  $\Xi_c^+ \rightarrow \Xi^-\pi^+\pi^+$  signals with each of the cuts used in the analysis was investigated and compared to the Monte Carlo predictions. Also, split samples studies were performed which included separation into two different run periods, into particle and anti-particle, and into high and low momentum for the heaviest daughter particle. We checked that the results were consistent for different topologies for the reconstructed  $\Xi^-$  hyperons and for different histogram binning and fit conditions. The results were compatible within errors with the quoted branching ratio. From all these studies, summarized in Figure 3 and in Table 1, we estimate an upper limit to the systematic error to be 0.022.

We have further investigated the resonant components of the  $\Xi_c^+ \rightarrow pK^-\pi^+$  decay. Figure 4 (a) shows the Dalitz plot obtained for a value of  $\ell/\sigma_\ell > 10$ . In the plot it is possible to recognize the presence of the  $\bar{K}^*(892)^0$  meson. Due to the relatively high background level the resonant components have been evaluated from the sideband subtracted two-body invariant mass spectra. No structures compatible with  $\Delta$  resonances have been observed (Figure 4 (b)), while we observe structures of excited hyperons in the regions around  $1.6 \text{ GeV}/c^2$  and at the edge of phase space around  $2.25 \text{ GeV}/c^2$  as shown in Figure 4 (c). However, they are not stable enough against variations in the analysis cuts and changes in the selection of sideband regions for us to quote branching fractions for them. Thus we limited our consideration to the resonant component of the  $\Xi_c^+ \rightarrow pK^-\pi^+$  where the  $K^-$  and  $\pi$  form a  $\bar{K}^*(892)^0$  meson (Figure 4 (d)). The signal has been normalized using the value from the fitted three body invariant mass plot. All the fits were performed using Breit-Wigner distributions for the signals and linear backgrounds. The signal widths have been constrained to those predicted by the Monte Carlo. The Monte Carlo simulation indicated a small (6%) difference in efficiency between the resonant and non-resonant components of the decay which has been taken into account. We determine the branching ratio to be:  $\Gamma(\Xi_c^+ \rightarrow p\bar{K}^*(892)^0) * \text{BR}(\bar{K}^*(892)^0 \rightarrow K^-\pi^+)/\Gamma(\Xi_c^+ \rightarrow pK^-\pi^+) = 0.36 \pm 0.06$  (stat). Assuming Isospin conservation in the process  $\bar{K}^*(892)^0 \rightarrow K\pi$  we can correct this value for unobserved  $\bar{K}^0\pi^0$  decays, thus we get:  $\Gamma(\Xi_c^+ \rightarrow p\bar{K}^*(892)^0)/\Gamma(\Xi_c^+ \rightarrow pK^-\pi^+) = 0.54 \pm 0.09$ (stat). The consistency of the result has been tested using different sets of tighter cuts and different choices for the sidebands. Using the fit variant method on the obtained result we estimate an upper limit to the systematic error to be 0.03 when only charged decays are considered and 0.05 after the correction for the neutral process are taken into account.

In conclusion we determine the branching ratio of the Cabibbo suppressed channel  $\Xi_c^+ \rightarrow pK^-\pi^+$  with respect to the Cabibbo favoured mode  $\Xi_c^+ \rightarrow \Xi^-\pi^+\pi^+$  to be:

$$\text{BR} \frac{(\Xi_c^+ \rightarrow pK^-\pi^+)}{(\Xi_c^+ \rightarrow \Xi^-\pi^+\pi^+)} = 0.234 \pm 0.047(\text{stat}) \pm 0.022(\text{syst}).$$

This result is in good agreement with SELEX measurement [1],  $\text{BR}(\Xi_c^+ \rightarrow pK^-\pi^+)/\text{BR}(\Xi_c^+ \rightarrow \Xi^-\pi^+\pi^+) = 0.20 \pm 0.04 \pm 0.02$ . We measure the relative branching ratio  $\text{BR}(\Xi_c^+ \rightarrow p\bar{K}^*(892)^0)/\text{BR}(\Xi_c^+ \rightarrow pK^-\pi^+)$ :

$$\text{BR} \frac{(\Xi_c^+ \rightarrow p\bar{K}^*(892)^0)}{(\Xi_c^+ \rightarrow pK^-\pi^+)} = 0.54 \pm 0.09(\text{stat}) \pm 0.05(\text{syst})$$

and detect the presence of  $(Kp)$  hyperon formations, but no evidence of  $\Delta$  isobars.

We wish to acknowledge the assistance of the staffs of Fermi National Accelerator Laboratory, the INFN of Italy and the physics department of the collaborating institutions. This research was supported in part by the U. S. National Science Foundation, the U. S. Department of Energy, the Italian Istituto Nazionale di Fisica Nucleare and Ministero dell'Università e della Ricerca Scientifica e Tecnologica, the Brazilian Conselho Nacional de Desenvolvimento Científico e Tecnológico, CONACyT-México, the Korean Ministry of Education, and the Korean Science and Engineering Foundation.

## References

- [1] SELEX Collaboration, S.Y. Jun et al., *Observation of the Cabibbo-suppressed decay  $\Xi_c^+ \rightarrow pK^-\pi^+$* , Phys. Rev. Lett. **84**, 1857 (2000).
- [2] FOCUS Collaboration, J.M. Link et al., *A measurement of lifetime differences in the neutral  $D$  meson system*, Phys. Lett. **B485**, 62 (2000).
- [3] E687 Collaboration, P.L. Frabetti et al., *Description and performance of the FERMILAB E687 Spectrometer*, Nucl. Inst. and Meth in Phys. Res., **A320**, 519 (1992).

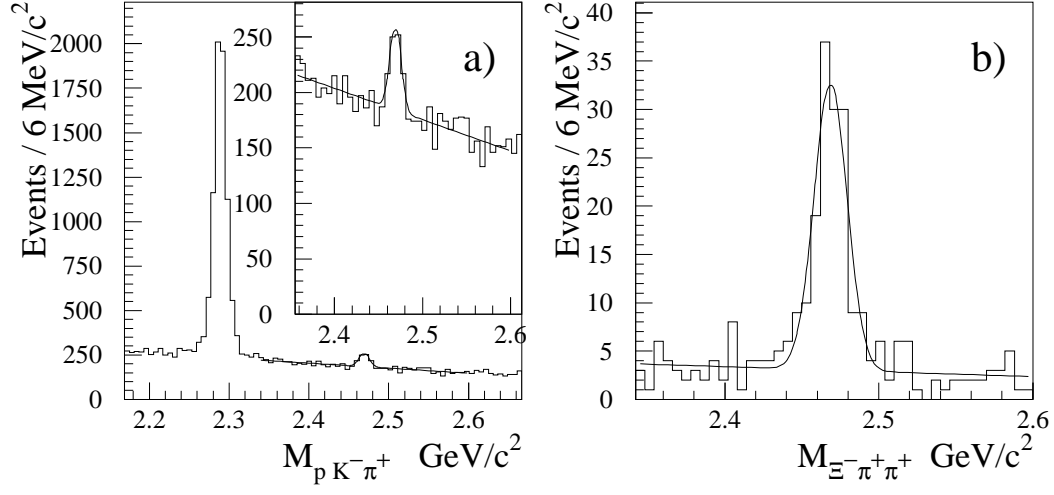


Fig. 1. Invariant mass distributions: a)  $pK^-\pi^+$ ; b)  $\Xi^-\pi^+\pi^+$ .

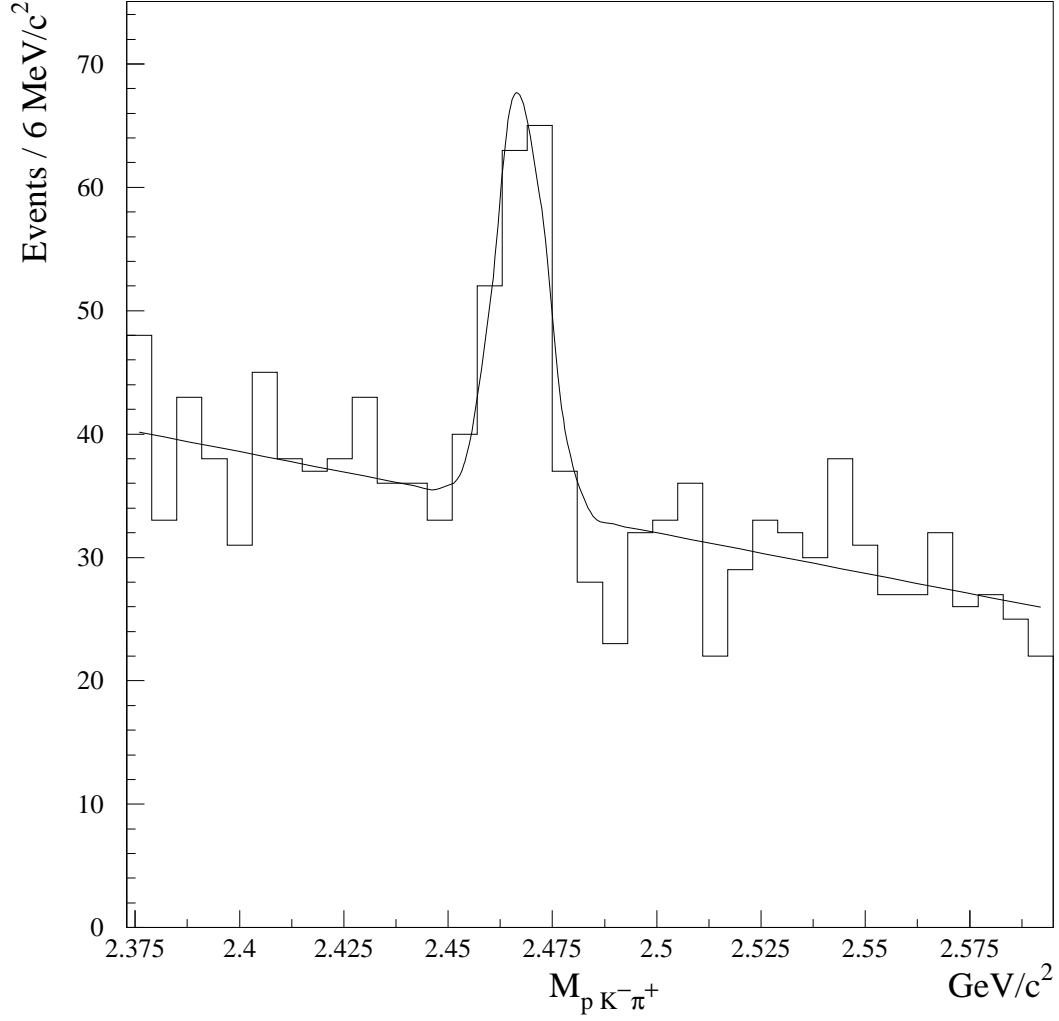


Fig. 2. Invariant mass distribution for the  $\Xi_c^+ \rightarrow pK^-\pi^+$  candidates

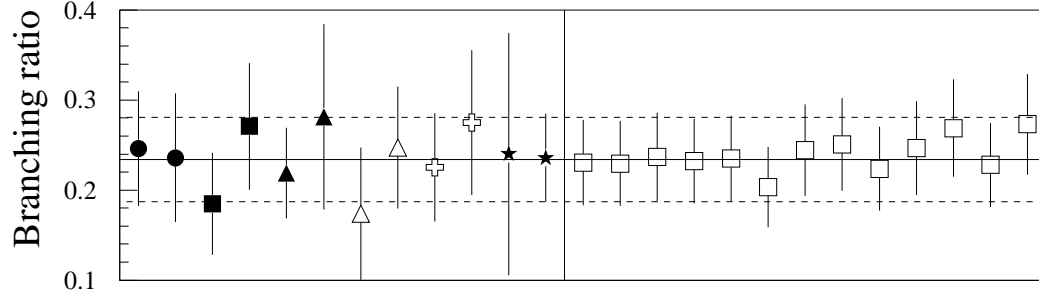


Fig. 3. Systematic studies summary: split samples and fit variants. First 12 points refer to the split sample test: high and low charm baryon momentum; high and low heaviest daughter momentum; earlier and later runs; upstream and downstream target region; particles and anti-particles; low and high value of detachment significance  $\ell/\sigma_\ell$ . The other 13 points demonstrate the stability versus: different binning (points 13 through 16); different fit intervals (points 17 through 25); and different background functions (linear for points 17 through 19, second order polynomial for points 20 through 22, and third order for points 23 through 25).

Table 1

Contributions to the systematic uncertainty for the measured branching ratio.

Split sample	0.0000
$\Xi^-$ topology	0.0018
Fit Variant	0.0216
Total systematic error	0.0223



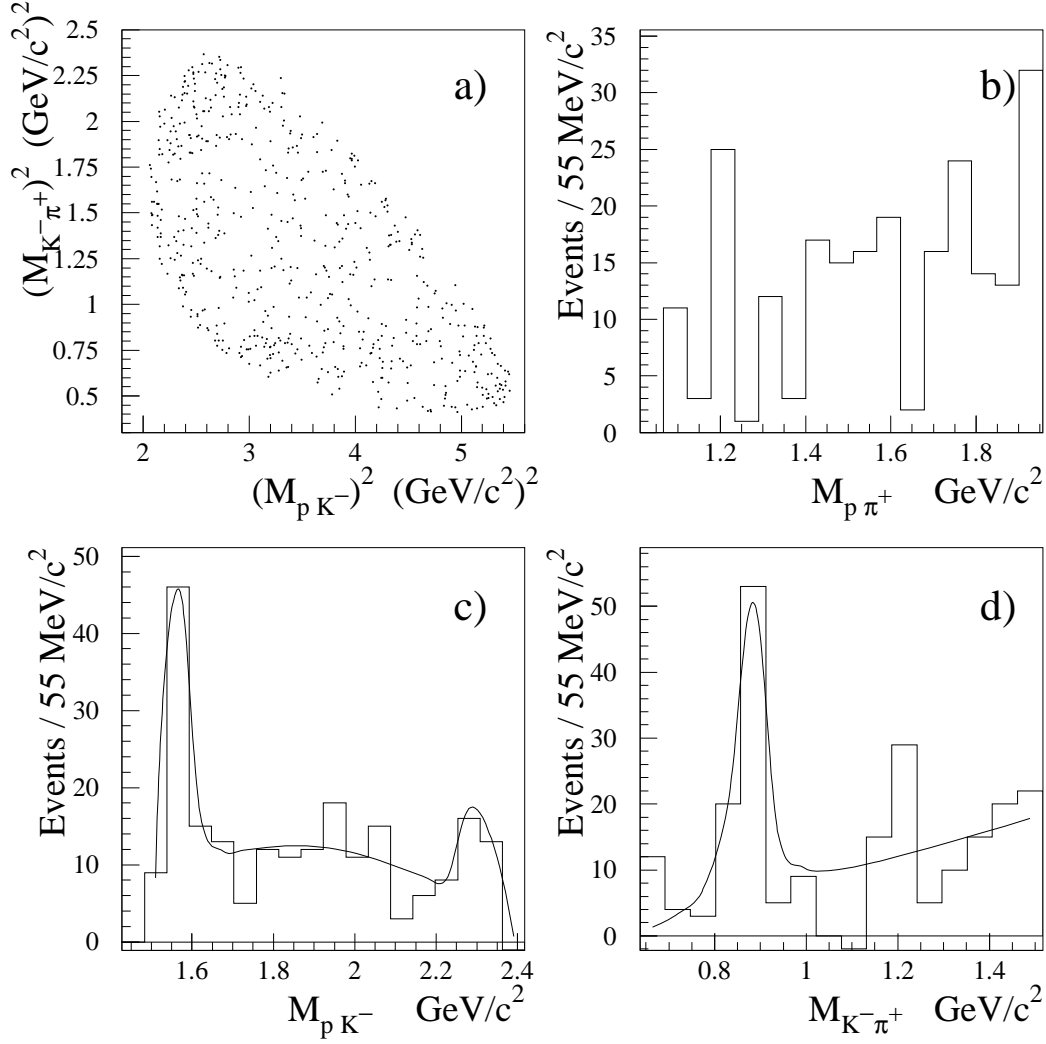


Fig. 4. Analysis of resonant structure: a) Dalitz plot for the  $\Xi_c^+ \rightarrow p K^- \pi^+$  process; b) 2 body invariant mass distribution for the proton pion system; c) 2 body invariant mass distribution for the proton kaon system; d) 2 body invariant mass distribution for the kaon pion system.